EFFECT OF FIBER BED ARCHITECTURE ON SINGLE RESIN DROPLET SPREAD FOR PREPREG MANUFACTURING

Patricio Martinez, Bo Jin, Steve Nutt University of Southern California 3651 Watt Way, VHE-412 Los Angeles, CA 90089

1. ABSTRACT

Previous studies have shown how discontinuous resin formats can increase the robustness of Vacuum Bag Only (VBO) prepregs. Current formats of this discontinuous resin format, dubbed USCPreg, all rely on a discontinuous film being applied on a fiber bed using only pressure. However, efforts are currently being undertaken to apply the discontinuous resin to the fiber bed directly, without a separate filming step. These methods should allow broader and more diverse characteristics of the prepreg, and allow a reduction in bulk factor, customization of the resin distribution, and potentially enable the production of prepreg "on demand."

To understand how applying discontinuous resin to a dry fiber bed at temperatures suitable for resin deposition may affect the final distribution, small-scale experiments were conducted. A fluid with controlled viscosity, matching the viscosity of epoxy resin during hotmelt processing, was used to minimize variability. The experiments consisted of a sessile droplet of facsimile fluid being deposited on the surface of a single ply of reinforcement. The spread of the fluid was then recorded, using a goniometer as well as a standard camera. Post-processing of these recordings was performed to obtain the spreading of the fluid in three directions: in the plane directions and the out-of-plane direction. The fluid was constant, a 30Pa.s rheological standard, but the reinforcement was varied to determine how the fluid interacted with different reinforcements. Macro-scale changes, such as fabric weave and fabric areal weight, and micro-scale parameters, such as tow width and fiber size, were varied to observe their effects on fluid distribution

The experiments yielded maximum in-plane spread distance, time for the resin to fully impregnate into the fibers, and aspect ratio of spreading, particularly for non-symmetric weaves. The results can be used to guide how the resin is deposited on different reinforcements, in order to achieve a resin distribution that will consistently yield high-quality parts. In addition, it is possible these observations can be applied to resin flow in standard continuous film prepreg, such as predicting the final degree of impregnation.

2. INTRODUCTION

2.1 Motivation – Development of High Through-Thickness Permeable Prepreg

Work within USC has shown the value of discontinuous resin out-of-autoclave prepregs format, which allows for through-thickness permeability [1]. Studies have shown that this experimental prepreg, dubbed USCPreg, is resistant to variations from standard processing conditions and that the specific resin distribution used can vary part quality and robustness [2]. Furthermore, the decrease in breathe-out pathway distance results in decreased porosity [3]. This material,

however, is not a silver bullet, and a previous study revealed that the method currently used to manufacture it results in a high bulk factor [4].

Current work into this prepreg is looking into improving the bulk factor, which occurs due to the low degree of impregnation [5]. Methods include the potential of dispensing droplets of resin on the surface of the prepreg at an elevated temperature. The elevated temperature of the resin would decrease viscosity and allow for partial impregnation. Comparing this to the current methods of manufacture, which rely on a separately prepared discontinuous resin film being pressed onto the fiber bed at room temperature: the resin is adhered to the fiber bed surface, but not impregnated [2][4][5].

This study was undergone to understand how small amounts of resin flow on carbon fiber bed, whether it be droplets deposited on the surface or simply heating the discontinuous film after the standard cold pressing. Specifically, in this paper the focus is on non-unidirectional fabric weaves and the effect that the relatively large-scale features of the fabric have on resin flow.

While unidirectional fiber beds may be the most used in standard aerospace industry prepregs, the flexibility of the prepreg manufacturing should allow for a variety of fabric types, and this study aims to understand the differences between the different fabric types.

2.2 Background – Droplets on a Porous Surface

Work on the flow of droplets on surfaces is extensive, with evidence showing the governing forces are gravitational forces, surface tension, and viscous forces, with small droplets allowing for neglecting of the gravitational forces [6][7][8]. Furthermore, on porous surfaces, capillary effects must be considered as well [9][10].

One of the main differences between this study and prior work is that most porous surface droplet flow studies work on the assumption that the material is isotropic and that the pores are represented by cylinders perpendicular to the surface [11]. Carbon fiber beds are anisotropic, and the permeabilities in the directions perpendicular and parallel to the fibers can vary by orders of magnitude [12]. This heterogeneity is further emphasized for non-unidirectional fabric weaves, where on the small-scale individual tows may behave like unidirectional fabric, but the specific fabric architecture is of note on the larger scale.

It is worth noting that there is a study on fluid droplet flow on a fiber bed surface [13]. However, this study uses a very low fluid viscosity (0.38 Pa-s), which is a viscosity suitable for full fabric impregnation, and not the prepreg preparation for which this study is developed.

2.3 Goals

The main goal of this study is to experimentally observe the effects of the macro-level details of a variety of fiber beds on the spreading of fluid on the surface. Particularly, details such as tow edges, overlaps/underlaps, and pinholes will be observed. These will be compared to fluid flow on a unidirectional fiber bed as well.

The following parameters will be measured: height of the droplet above the fabric surface over time, surface area coverage over time, and the shape of surface coverage over time. As this is an

empirical study, observations of these parameters will be made, but no specific model or analytical predictions will be developed.

3. EXPERIMENTAL METHODS

3.1 Materials - Fluid Selection

While the motivation behind this study is to understand the flow of resin on the fiber bed surface, working with resin and controlling its viscosity carefully can be difficult, in this case requiring carefully controlling the temperature of the resin reservoir, the fiber bed, and the air through which the droplet travels. Therefore, a facsimile fluid is selected instead.

The resin of choice for the previous iterations of USCPreg [3-5] was selected as the basis for this study as well. This is an epoxy resin developed by Patz Materials & Technologies (PMT-F4A). Using the suppliers filming procedure, the minimum viscosity achieved during deposition was obtained. Per the supplier, the filming temperature cycle is the following: Resin is pre-melted at 65-68°C (150-155°F) for 30-60 minutes. Then, filming is done at 68-72°C (155-162°F), which takes 30 minutes. Using a pre-filming sample of the resin provided by the supplier, a rheology test was done following the maximum temperatures allowed within this cycle and can be seen in Figure 1.

From this test, the minimum viscosity value during the filming process was found to be 27.1Pa-s. Therefore, a facsimile fluid of 30Pa-s was selected as it is the closest standard viscosity to the minimum achieved. The facsimile fluid selected is a silicone viscosity standard with a viscosity of 30Pa-s ($\pm 1\%$) (General Purpose Silicone, Brookfield Ametek). This fluid is ideal for these tests, as it the variation in viscosity due to the temperature at values near room temperature are a minimum.

It is worth noting, however, that the fluid is transparent, and in further studies, attempts will be made at either obtaining a colored fluid or dying the viscosity standard, as the transparency leads to difficulties in observation of the fluid.

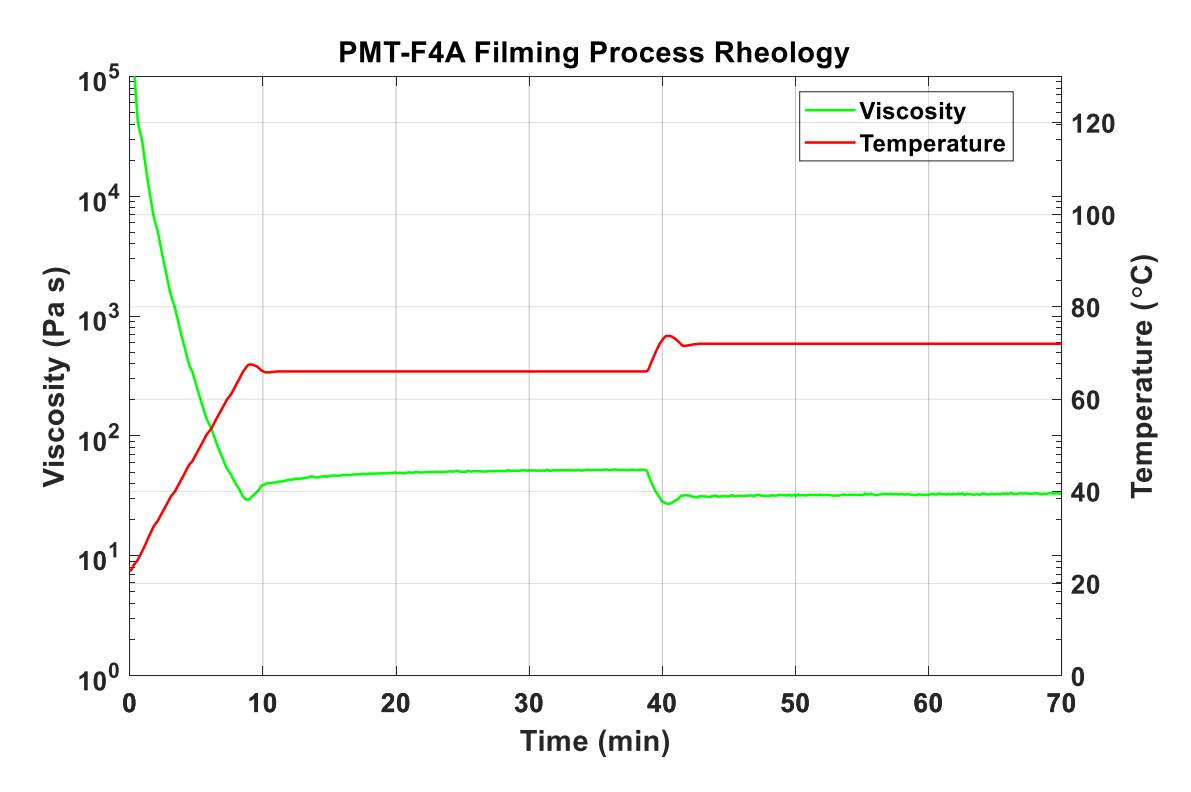


Figure 1: Rheology test for an un-filmed sample of PMT-F4A, following the filming process thermal cycle at the highest temperatures allowed.

3.2 Materials – Fabrics

The baseline fiber bed, for which the others will be compared to, will be a 305gsm (9.0 oz/sq.yard) unidirectional non-crimp fabric (UD-NCF). This fabric was selected as it is currently the fabric of choice for manufacturing through-thickness permeable prepreg [2][4][5]Alongside this, three different weaves were also selected: A plain weave (PW) fabric with an areal weight of 119 gsm (3.5 oz/sq.yard); a 2x2 twill (TW) fabrics with areal weights of 193 gsm (5.7 oz/sq.yard) and two other unidirectional fabrics, a 137 gsm (4.0 oz/yard) matching the 305gsm UD-NCF, and a heavier 756 gsm (22.3 oz/sq. yard) quilted unidirectional fabric.

These fabrics were purchased from Fibre Glast (Products #2583, #2363, #1069, #1073, #2585, #2595).

Fabric properties are outlined in Table 1. Pictures of each of the six fabrics are shown in Figure 2.

Table 1: Fabric Properties

	Fabric Style	Areal Weight	Tow Count
		$[g/m^2]$	[-]
1	UD-NCF	305	24K
2	UD-NCF	136	12K
3	TW	193	3K
4	PW	119	1K
5	Quilted UD	756	24K

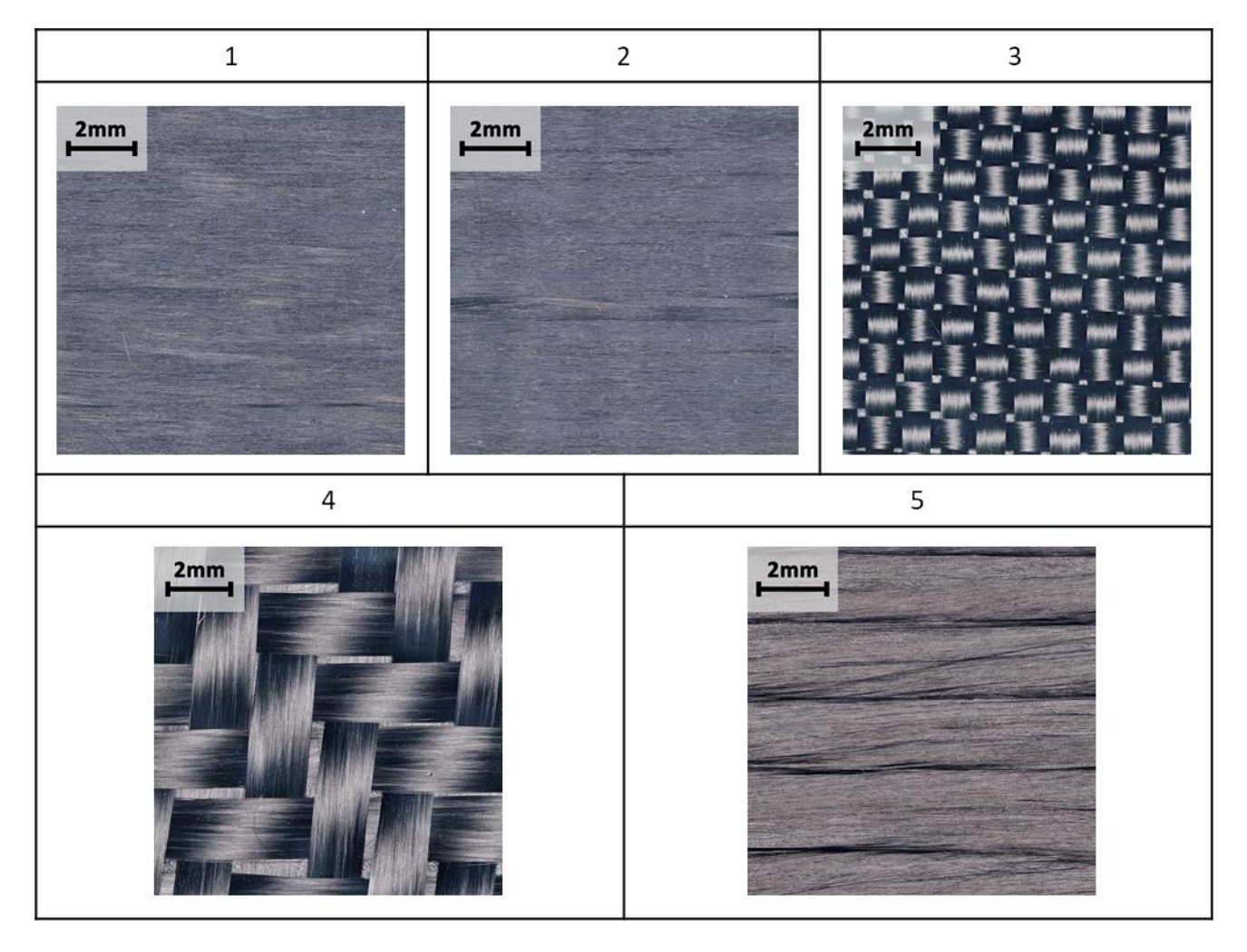


Figure 2: Close up images of the corresponding fabrics in Table 1

Looking at Figure 2 the main features of the different fabrics become apparent: The UD-NCF samples (Fabrics 1 and 2) are smooth and uniform throughout. The PW sample (Fabric 3) is fairly uniform with its weave, and the weave is tighter than the TW samples, with the pinholes being the only regions through which the bottom surface can be seen. The TW sample (Fabric 4) has a looser weave than the PW sample, with neighboring parallel tows not always touching. Finally, the Quilted UD sample (Fabric 5) also has some of the uniformity of the UD-NCF samples, except for being collected in distinct tows, providing tow edges to break the uniformity.

3.3 Testing Methodology

Testing is split into two sections: First, surface topology mapping, and second the actual droplet deposition test.

3.3.1 Surface Topology Mapping

Fabric samples are prepared by securing a 25.4 by 25.4 mm (1 by 1 in) section with tape and then cutting the square out. Edges are secured with tape to prevent frayed edges from lifting up and ruining the fabric.

A 3D image of the surface is obtained using an optical microscope (VHX-5000). The microscope image generates 3D data used to create a topographical map, as well as a 150x image. Cropped versions of these images are used in Figure 2. An example of the topographical map is shown in Figure 3.

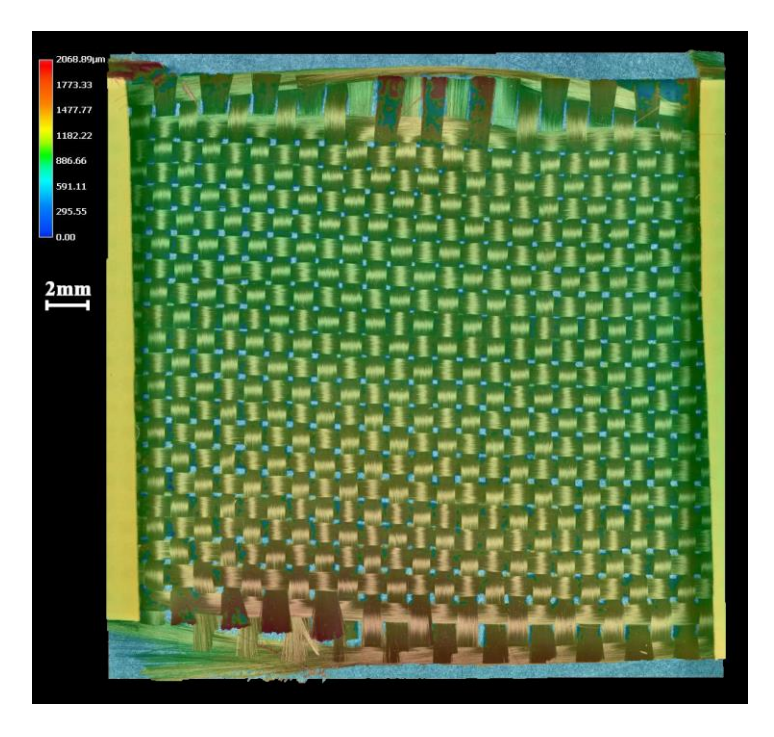


Figure 3: Topographical image of the plain weave fabric.

The topographical mapping will be used to obtain a more concrete measure of the variation in surface uniformity and roughness that arises from the different weaves. A pinhole is a much more severe height difference than a tow over/underlap, as can be seen in the figure above.

3.3.2 Droplet Deposition Test

The droplet deposition test is the main way in which data was gathered for this test. Two separate views of the droplet were recorded with separate devices. A goniometer (Ramé-Hart Model 500) was the main device used during this test, providing the stage for the fabric sample, as well as the syringe system for dispensing a droplet. The fabric sample was secured to the goniometer stage with tape along the edges to ensure the sample remains flat.

The goniometer recorded a side view of the droplet, while a digital camera (LUMIX GH4) was used to record the top view. A syringe was used to deposit a 5mL droplet onto the fabric, at with both recording devices starting to record once the droplet began falling under its own weight.

Images were recorded every two seconds by the goniometer and every ten seconds by the top-down camera. These two sets of images were separately analyzed. An example of these images can be seen in Figure 4.

The data gathered from each of the views is the following: The side view allows for measuring the height of the droplet that is above the fiber bed surface. The top-down view is used to measure the area being covered by the droplet over time.

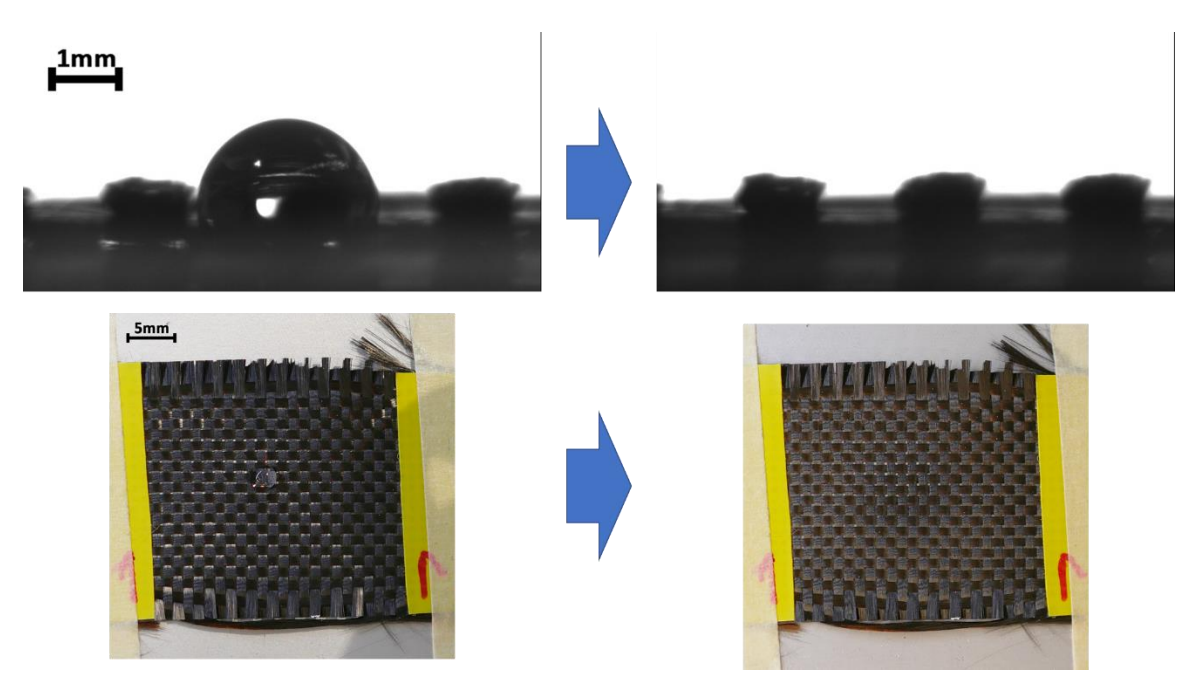


Figure 4: Images captured during the droplet deposition test for the plain weave fabric sample. Side view images (above) are taken with the goniometer, while top-down images (below) are taken with a camera. The images on the left are immediately following deposition, while those on the right are after 1000 minutes, at the end of the test.

4. RESULTS

4.1 Height over Time

The height of the droplet over time is measured using an automated MATLAB script. Given that the goniometer images are output in greyscale, such measuring is simple to do. Using the final image in the sequence, a baseline for the final height is set, and then for each individual image, the height of the droplet is compared to that.

A measure of the height over time was determined to be the time it takes for the height to stop changing. While ideally, this would be the time it takes for the height to reach zero, in some cases the droplet never is fully absorbed into the fabric, particularly for the lighter areal weight fabrics. This time will be referred to as the time to full absorption (t_{h0}) .

The results for the height over time data can be seen in Figure 5. Given the majority of the data occurs at the beginning of the graph, and the power-function form of the curves, the data is also plotted against the logarithm of time in Figure 6.

The general shippe of the height vs time curves follows a power-function, which matches previous studies on the spreading of a droplet on a solid surface [6].

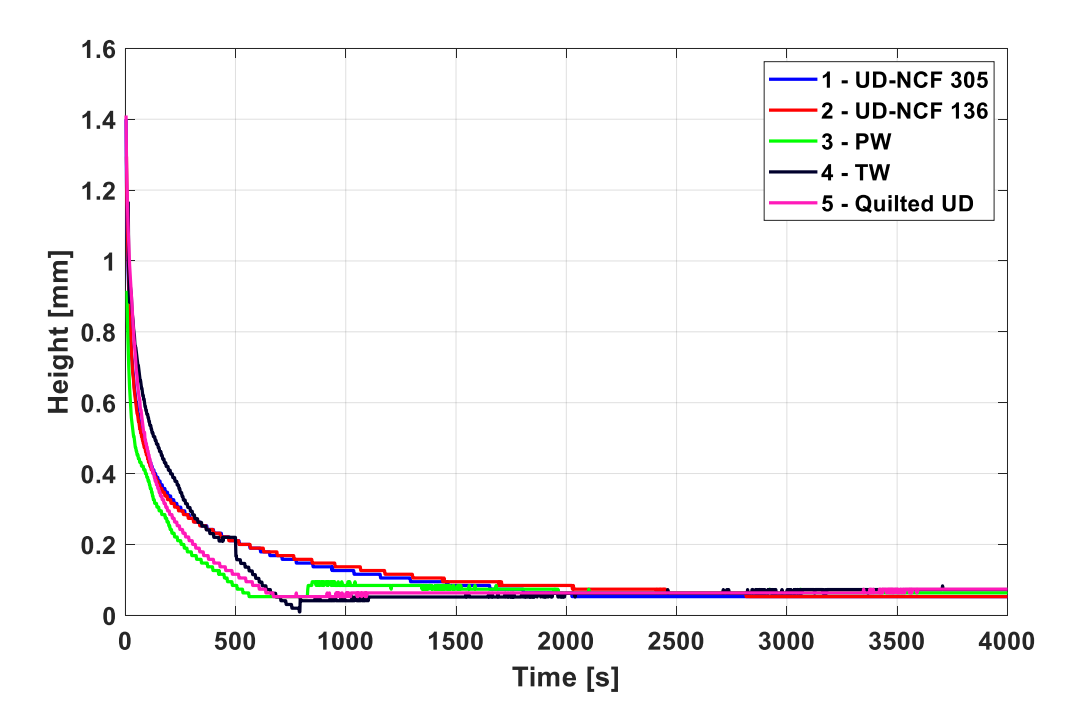


Figure 5: Height vs Time data for all five fabric samples

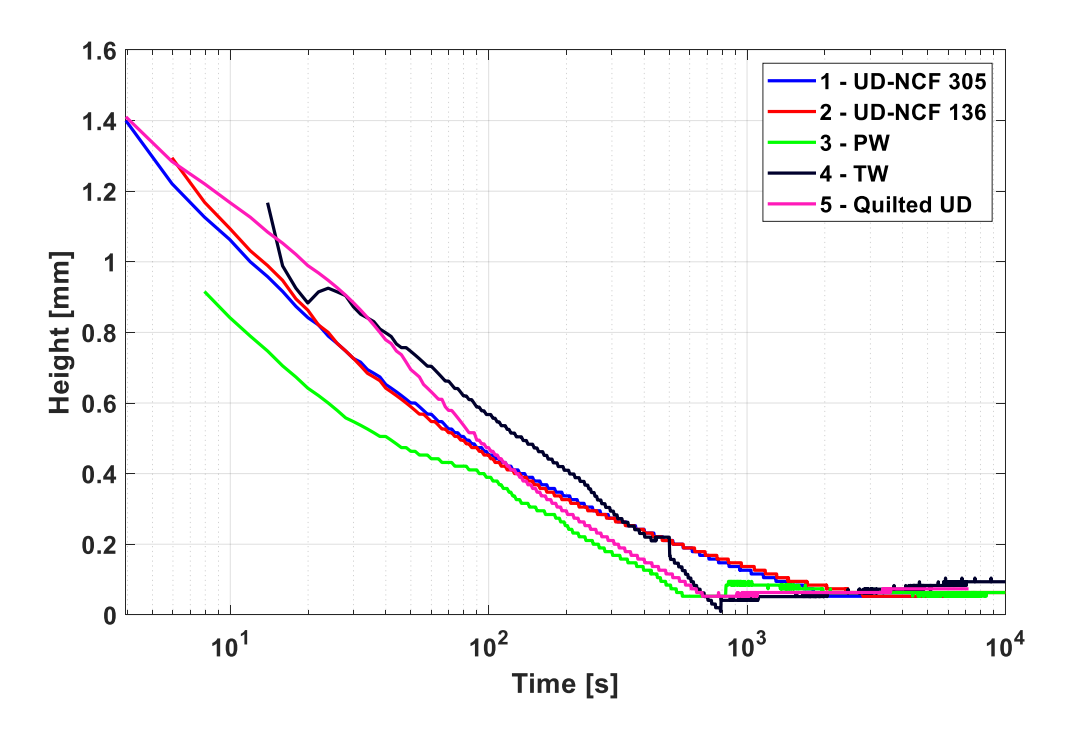


Figure 6: Height vs Time data, plotted with a logarithmic scale for time.

One thing worth noting, that is difficult to make out clearly from the graph is that the two UD-NCF fabrics follow a very similar height curve, with the only significant difference of note being a difference in the time to full sorption.

The time to full sorption for each fabric sample was measured, recorded as the time where height stopped changing. These values are outlined in Figure 7. Of note is the significant difference from the standard UD-NCF samples to the woven fabrics. This was expected, following the fact that the non-UD samples have a significant number of pores and gaps in the fiber bed surface that are much larger than the small capillaries that form between individual tows in the unidirectional fiber beds.

Looking at the two UD-NCF fabrics, the difference in time to full sorption can be correlated to fiber areal weight: The heavier fabric, sample 1, allows more fluid to flow in the out-of-plane direction before reaching full saturation.

Between the three non-unidirectional weaves, the fastest time to full sorption is for the plain weave fabric. This is likely due to the high number of pinholes, and how the pinholes provide full clearance between the top and bottom of the fabric.

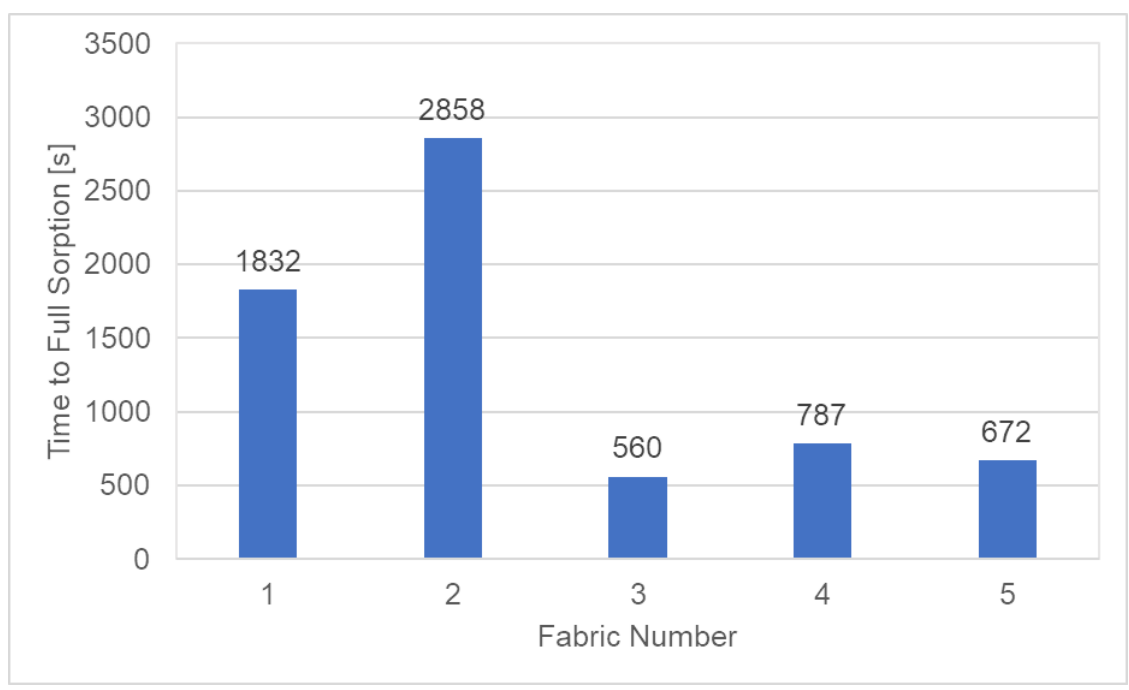


Figure 7: Bar graph showing the time to full sorption for all five fabric types.

4.2 Surface Coverage over Time

Using the top-down view, the area covered by the droplet was measured. This was done by selecting images at specific points in time and manually covering the droplet, then using the image processing code to determine the covered area. Due to lighting difficulties, some data points are missing. Furthermore, the droplet became absorbed into the fabric for some weaves, becoming too faint to be measured. The surface area vs time data is shown in Figure 8.

Some things to note from this data is that, much like the height vs time data, the two UD-NCF samples followed a very similar curve, with both having the surface area covered continue to expand over time until the time of test termination (t=10000s). The other weave styles exhibited a maximum coverage value before the surface area covered began to decrease, as the droplet became fully absorbed into the fabric.

This behavior is expected for fluid flow over porous media, where the wetting phenomena of a droplet on a surface drive the surface area covered to increase, while the capillary effects of the porous surface drive fluid into the material, causing the covered area to decrease [18].

In the case of the UD-NCF fiber beds, the capillary effect is significantly lower due to the smaller size of the capillaries, resulting in the time needed to observe the maximum surface coverage exceeding testing time.

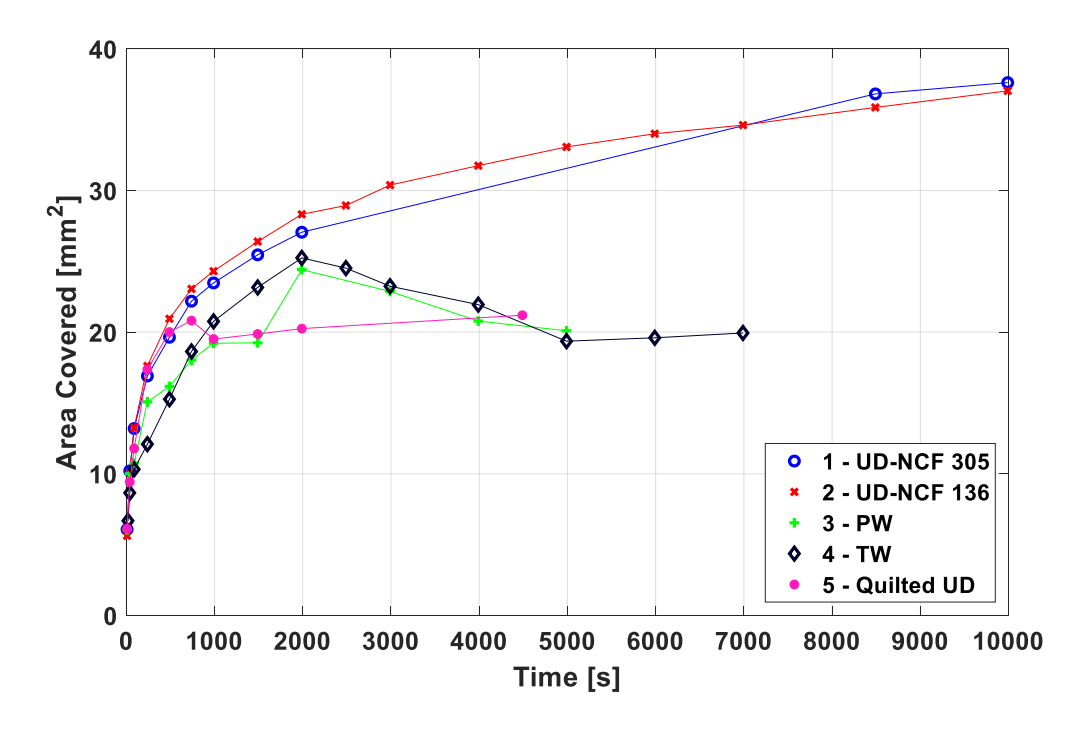


Figure 8: Surface area covered by fluid over time for the different fabric samples.

The effect of each individual weave, however, is better seen by the shape the fluid takes when covering the droplet, and not merely the value of the coverage that Figure 8 shows. For this, Figure 9 shows a general guideline, displaying contours of the droplet over time.

What the contours show is that the fluid follows the details of the weave closely: for the UD-NCF fabrics it spreads mostly along the direction parallel to the fibers; for PW the fluid flows around the pinholes, until it wraps around the pinhole and goes over; the TW sample shows the fluid unable to go over the sides of tows and flow into the tow edges; this same behavior can be seen in the Quilted UD sample, where the fluid spreads significantly in the gap between two adjacent tows.

In the case of the plain weave fabric, it is predicted that the droplet was large enough that positioning would not affect the spread significantly, the ratio of droplet size to weave detail size was large. However, for the other two woven fabrics, the size of the weave details is significant compared to the size of the droplet. Looking particularly at the Quilted UD sample, the droplet is positioned directly in the boundary between two tows and spreading of the droplet follows the boundary line closely, with even less spreading across the fibers than the other unidirectional cases, as the droplet is absorbed between the two tows.

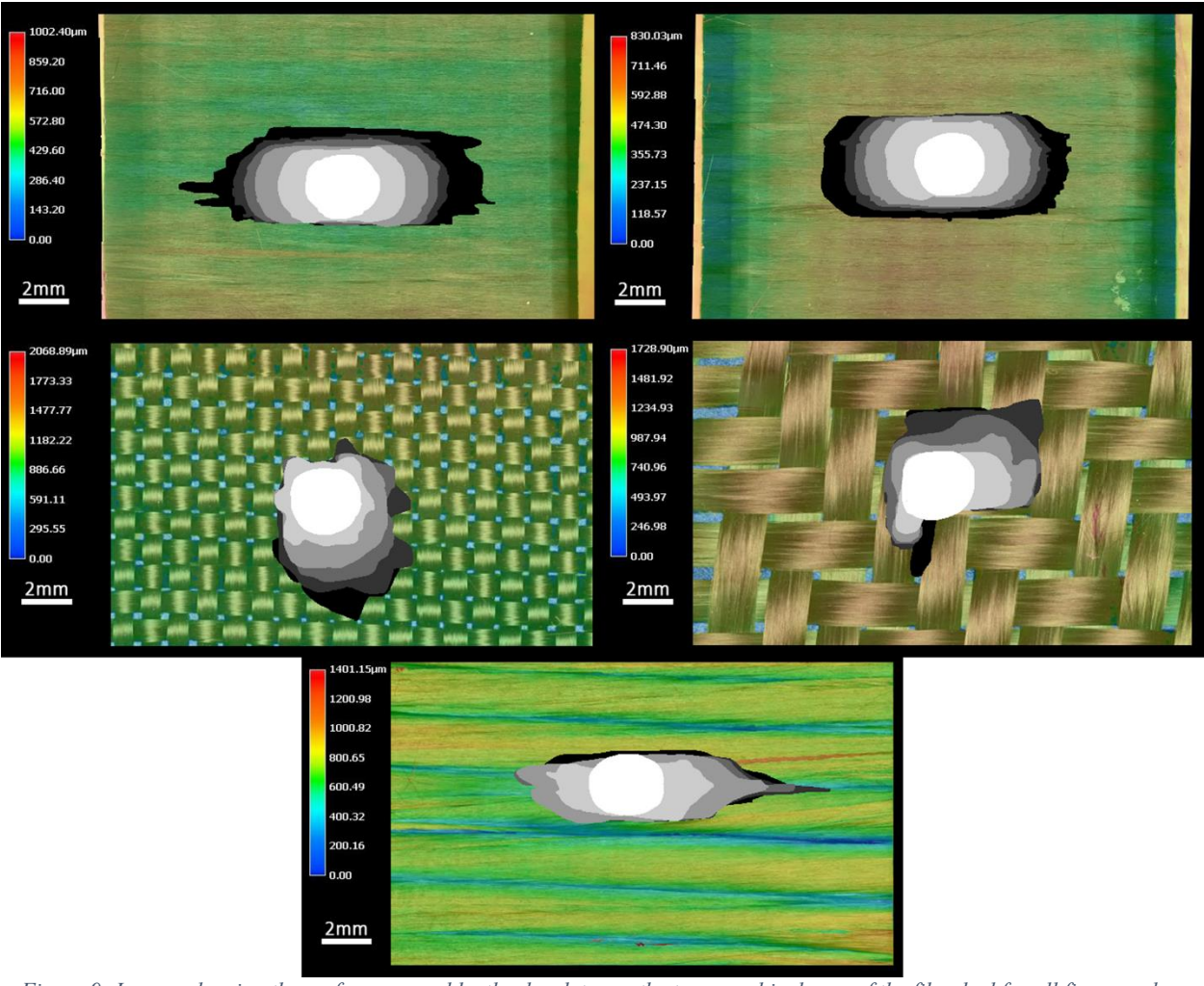


Figure 9: Images showing the surface covered by the droplet over the topographical map of the fiber bed for all five samples. Times of each contour are at 10, 100, 500, 1000, 2000 seconds after droplet deposition, as well as at the last moment at which the droplet can be observed, as shown in Figure 8.

5. CONCLUSIONS

Based on the small number of tests performed for this paper, it can be clearly seen that the weave that is chosen for the fiber bed significantly affects the overall shape of the droplet as it spreads. Unidirectional fiber beds display a spreading that is dominated by the direction of the fibers. Plain weave exhibits nearly uniform spreading, except for the pinholes, which divert flow momentarily. Twill weave, however, inhibits spreading of the fluid along the surface, the rougher surface than plain weave preventing proper flow along the surface.

The fact that the plain weave fabric used in this study is particularly lightweight and has a tight weave and small tow size when compared to the twill weave fabric shows the importance of fiber bed detail size when compared to droplet detail size. If the droplets are large enough, it is possible that a weave such as a twill can result in full droplet spreading.

Yet another factor that shows the importance of fiber weave for droplet spreading and imbibition is the fact that using a fabric with half the areal weight did not significantly change the results

observed for the UD-NCF samples. In both "height vs time" and "area-covered vs time", both UD-NCF samples exhibited nearly identical behavior, with a minor difference in time to full sorption being the only significant difference between them.

5.1 Future Work

A separate study is already underway, looking deeper into the effect of fabric areal weight and surface flow, as was seen in this study between the two UD-NCF samples.

Furthermore, this study was observing only fluid on and above the surface, with the flow within the fiber bed being unobserved. Given that the original motivation behind this study is to increase the degree of impregnation of discontinuous reservoirs of resin, observation of the subsurface flow, and of the degree of impregnation are yet another area of study that should be considered.

The relationship between fluid flow and fiber bed geometry is still not fully understood, and this paper was only a small stepping stone towards that goal.

6. REFERENCES

- [1] L. K. Grunenfelder, A. Dills, T. Centea, and S. Nutt, "Effect of prepreg format on defect control in out-of-autoclave processing," *Compos. Part A Appl. Sci. Manuf.*, vol. 93, pp. 88–99, 2017.
- [2] S. G. K. Schechter, T. Centea, and S. R. Nutt, "Polymer film dewetting for fabrication of out-of-autoclave prepreg with high through-thickness permeability," *Compos. Part A Appl. Sci. Manuf.*, vol. 114, no. May, pp. 86–96, 2018.
- [3] T. A. Cender, P. Simacek, S. Davis, and S. G. Advani, "Gas Evacuation from Partially Saturated Woven Fiber Laminates," *Transp. Porous Media*, vol. 115, no. 3, pp. 541–562, 2016.
- [4] P. Martinez and S. R. Nutt, "Robust Manufacturing of Complex-Shaped Parts Using Out-of-Autoclave Prepregs with Discontinuous Formats," in *CAMX*, 2018.
- [5] W. T. Edwards and S. R. Nutt, "Out-of-Autoclave Prepreg Formats for Defect Control and Robust Processing," in *SAMPE*.
- [6] P. Neogi and C. A. Miller, "Spreading kinetics of a drop on a rough solid surfaces," *J. Colloid Interface Sci.*, vol. 92, no. 2, pp. 338–349, 1983.
- [7] L. M. Hocking, "The wetting of a plane surface by a fluid," *Phys. Fluids*, vol. 7, no. 6, pp. 1214–1220, 1995.
- [8] V. M. Starov, S. A. Zhdanov, and M. G. Velarde, "Spreading of liquid drops over thick porous layers: Complete wetting case," *Langmuir*, vol. 18, no. 25, pp. 9744–9750, 2002.

- [9] S. H. Davis and L. M. Hocking, "Spreading and imbibition of viscous liquid on a porous base," *Phys. Fluids*, vol. 11, no. 1, pp. 48–57, 1999.
- [10] S. H. Davis and L. M. Hocking, "Spreading and imbibition of viscous liquid on a porous base. II," *Phys. Fluids*, vol. 12, no. 7, pp. 1646–1655, 2000.
- [11] N. Alleborn and H. Raszillier, "Spreading and sorption of a droplet on a porous substrate," *Chem. Eng. Sci.*, vol. 59, no. 10, pp. 2071–2088, 2004.
- [12] S. Comas-Cardona, C. Binetruy, and P. Krawczak, "Unidirectional compression of fibre reinforcements. Part 2: A continuous permeability tensor measurement," *Compos. Sci. Technol.*, vol. 67, no. 3–4, pp. 638–645, 2007.
- [13] V. Michaud and A. Mortensen, "Infiltration processing of fibre reinforced composites governing: phenomena," *Compos. Part A Appl. Sci. Manuf.*, vol. 32, pp. 981–996, 2001.